The effect of N-methylation on photophysical properties of imidazole-based fluorescent molecules

Yao-Chun Yeh,[a] Lien-Chen Fu,[a] Wei Hsing,[a] Hsin-Chieh Lin,*[b] and Mei-Yu Yeh*[a]

[a]*Department of Chemistry, Chung Yuan Christian University, Zhongli Dist., Taoyuan City, Taiwan, Republic of China*

[b]*Department of Materials Science and Engineering, National Yang Ming Chiao Tung University, Hsinchu, Taiwan, Republic of China*
Email: hclin45@nycu.edu.tw myyeh@cycu.edu.tw

This article is dedicated to Prof. Tien-Yau Luh on the occasion of his 76th birthday

Abstract

Our research revealed that the introduction of a methyl group had a profound effect on the molecular geometry, resulting in a more twisted structure. As a consequence of this non-planar structure, the material exhibited aggregation-induced emission properties, making it a promising candidate for various practical applications. To support our findings, we used a range of analytical techniques, including UV-vis absorption spectra, fluorescence spectra, and theoretical calculations. This work provides valuable insights into the relationship between molecular structure and optical properties, which could inform the development of novel materials for a range of applications.
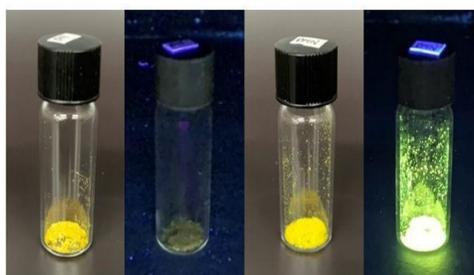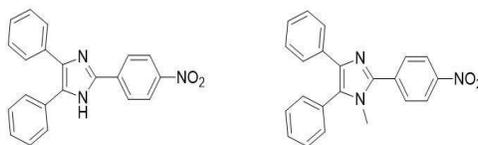
Introduction

The term aggregation-induced emission (AIE) was first proposed by Tang's research team in 2001, referring to fluorescent molecules that emit strong fluorescence in the aggregated or solid state, known as aggregation-induced emission luminogens (AIEgens).[1-3] These types of molecules have practical and wide-ranging applications, such as organic light-emitting diodes,[4,5] fingerprint recognition,[6-8] cell imaging,[9-12] environmental monitoring,[13] gas detection,[14-16] and so on. Over the years, numerous AIEgens have been developed, and in recent times, several research groups have formulated AIEgens of the donor-acceptor (D-A) type. These D-A type AIEgens exhibit an emission spectrum shifted towards longer wavelengths, which is highly advantageous for various fields of research.[17-22] Examples of such applications include highly efficient electroluminescent devices, bioimaging of living cells, sensing of volatile organic compounds, and other relevant uses.

Herein, we designed and synthesized a new type of imidazole-based D-A fluorescent molecules of **1** and **2** (Scheme 1), and explored the effect of the N-methyl substitution on the photophysical properties as well as molecular geometries. UV-vis absorption and emission spectra of **1** and **2** in different polarity solvents and solid powders were investigated. Additionally, we employed theoretical calculations to assist in comprehending the effect of N-methylation on the molecular structure and photophysics. The integration of experimental and theoretical calculation findings revealed that the methyl-substituted molecules exhibited a more twisted structure, ultimately leading to the material's AIE properties.
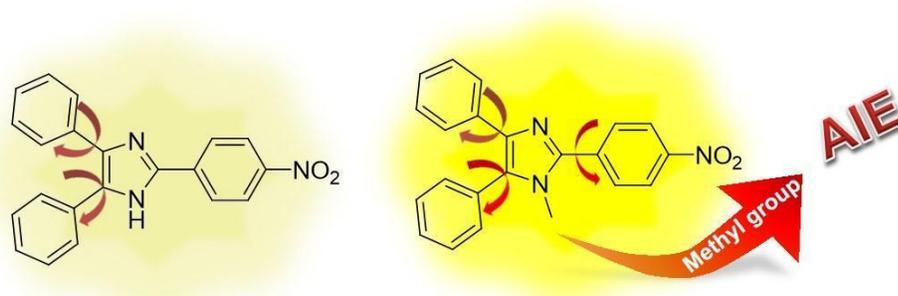
Scheme 1. The molecular design strategy of imidazole-based D-A fluorescent molecules of **1** (left) and **2** (right).

Results and Discussion

In this study, we aimed to examine the effect of N-methyl substitution on the photophysical properties of imidazole-based molecules, where the imidazole as the electron donor (D) and nitrobenzene as the electron acceptor (A). To achieve this, we designed and synthesized two novel compounds, **1** and **2**, which were then analyzed in different polar solvents and in the solid state. As shown in Scheme 2, compound **1** was synthesized using benzil, 4-nitrobenzaldehyde, and ammonium acetate with a yield of 96%. Subsequently, N-methylation of compound **1** resulted in compound **2** with a yield of 99%. Identification of the new compounds was carried out using ^{1}H nuclear magnetic resonance (NMR), ^{13}C NMR, and high-resolution mass (HR-Mass) spectrometry, with a comprehensive description of the relevant data included in the Experimental Section and Supplementary

Material. Overall, our study focused on investigating the photophysical properties of these newly synthesized molecules with a particular emphasis on the impact of N-methyl substitution.
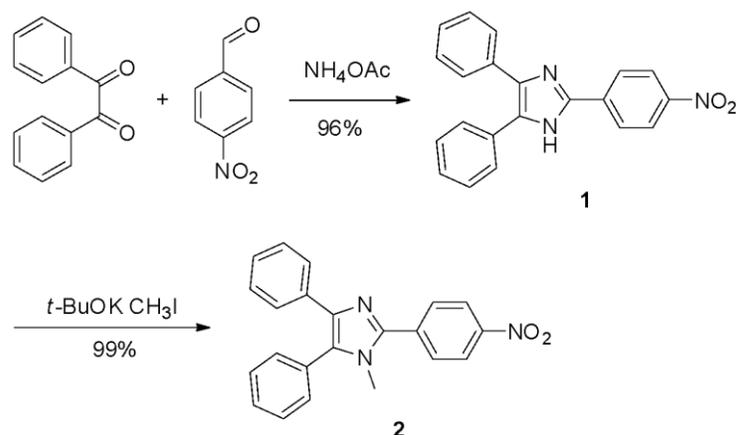
Scheme 2. Synthetic routes of compounds **1** and **2**.

To investigate the impact of the substituent effect on the molecule, we characterized the UV-vis absorption and fluorescence emission properties of **1** and **2** in solvents with varying polarities. As shown in Figure 1a and Table 1, the absorption bands of compound **1** at 50 µM in toluene, ethyl acetate (EA), and dimethyl sulfoxide (DMSO) were 387, 391, and 406 nm, respectively. The emission spectra were recorded using a range of excitation wavelengths, specifically 387 nm for toluene, 391 nm for EA, and 406 nm for DMSO. Figure 1b showed the emission wavelengths at around 501, 539, and 577 nm for **1** in toluene, EA, and DMSO, respectively. The experimental results revealed the presence of red-shifted emission wavelengths and diminished fluorescent signals in solvents with high polarity, suggesting the charge transfer occurring in compound **1**.[23-25] The absorption and emission spectra of compound **2** in different solvents were displayed in Figure 2, it was found that compound **2** exhibits photophysical phenomena with trends similar to those of compound **1**. Furthermore, compound **2** showed almost no fluorescence in DMSO. We further compared the Stokes shifts of compounds **1** and **2** in different solvents, and observed that the Stokes shifts of compound **2** were larger than those of **1** in the corresponding solvents, which could be attributed to the more twisted molecular structure of compound **2**.[26,27] In addition, for a given molecule, the larger the polarity of the solvent, the greater its Stokes shift (Table 1).
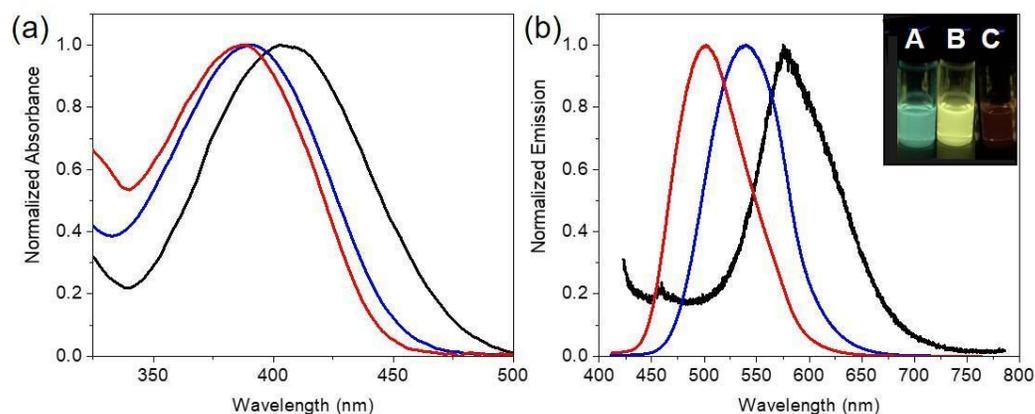
Figure 1. Normalized (a) UV-vis absorption and (b) fluorescence emission spectra of **1** at 50 µM in toluene (red), EA (blue) and DMSO (black). Insets are the photographs of solutions of **1** in (A) toluene, (B) EA and (C) DMSO, taken under UV irradiation at 365 nm.
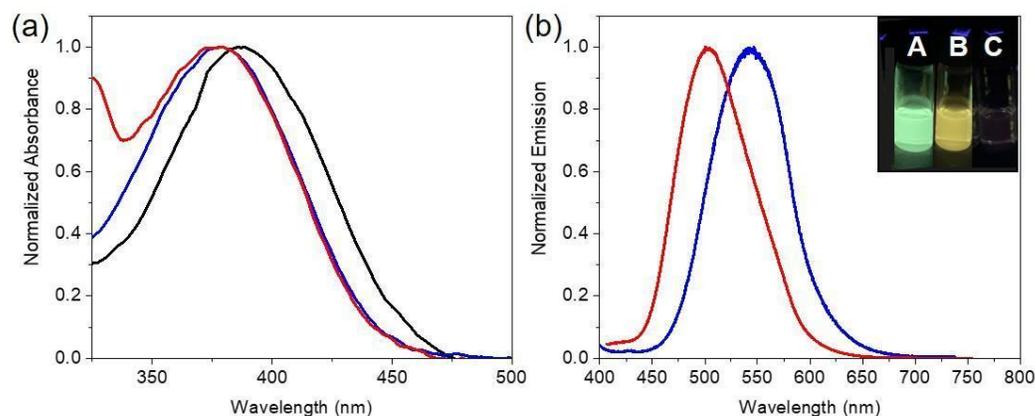
Figure 2. Normalized (a) UV-vis absorption and (b) fluorescence emission spectra of **2** at 50 µM in toluene (red), EA (blue) and DMSO (black). Insets are the photographs of solutions of **2** in (A) toluene, (B) EA and (C) DMSO, taken under UV irradiation at 365 nm.

Table 1. Photophysical properties of **1** and **2**

Compound	Solvent	λ_{max} (nm)	λ_{em} (nm)	$\Delta\lambda$ (nm)[a]
1	Toluene	387	501	114
	EA	391	539	148
	DMSO	406	577	171
2	Toluene	377	503	126
	EA	379	544	165
	DMSO	386	NA	NA

[a] Stokes shift. NA: not available.

Subsequently, we examined the solid-state properties of compounds **1** and **2** (Figure 3). Interestingly, we observed that **1** exhibited weak solid-state fluorescence under UV light, whereas **2**, which features a methyl substituent on the nitrogen atom, displayed intense fluorescence under UV illumination. This finding suggests that compound **2** may exhibit aggregation-induced emission (AIE) phenomena, thus, we carried out fluorescence spectroscopy analysis of **2** in toluene/DMSO mixtures with varying proportions.[28-30] As presented in Figure 4, the fluorescence intensity increased as the proportion of toluene increased, and there was a significant enhancement of fluorescence at a toluene proportion of 90%, with the highest fluorescence intensity observed at 95%. We speculated that this enhancement might be due to the π-π interactions between toluene and **2**, which could facilitate the aggregation of compound **2** and lead to strong fluorescence emission.[31,32]
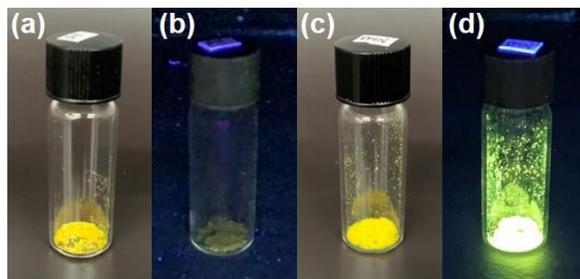
Figure 3. Images of the solid powder forms of (a, b) **1** and (c, d) **2** were captured in two lighting conditions: (a, c) ambient room lighting and (b, d) illumination with a 365 nm UV lamp.
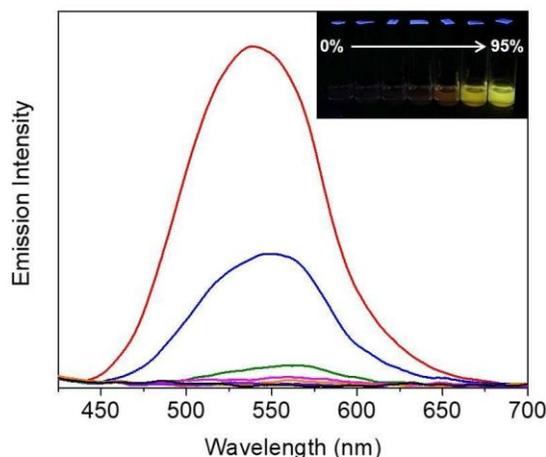
Figure 4. Fluorescence spectra of **2** at 50 μM in toluene/DMSO mixtures. (λ_{ex}= 386 nm) Inset: photographs of solutions of **1** in solvent mixtures of various toluene fractions (vol %), taken under UV irradiation at 365 nm. (red: 95%, blue: 90%, olive: 70%, magenta: 50%, orange: 30%, violet: 10%, black: 0%).

In order to further elucidate the properties of compounds **1** and **2**, we employed the M06-2X/6-31G(d,p) method to optimize their molecular structures using molecular modeling techniques.[33-35] In Figure 5, the highest occupied molecular orbital (HOMO) and lowest unoccupied molecular orbital (LUMO) diagrams of **1** and **2** were shown. Notably, the changes in the distributions of the HOMO–LUMO of **1** and **2** suggest the significant intramolecular charge transfer in both compounds. Additionally, the calculated energy gaps for **1** and **2** were found to be 5.34 and 5.37 eV, respectively, and these results are consistent with the observed absorption

spectra of **1** and **2** (Table 1). Figure 6 displayed the optimize structures of **1** and **2**, it was observed that the steric effect of the methyl substituent on the nitrogen atom of **2** causes a dihedral angle of 31.8° between the imidazole and nitrophenyl groups, indicating a more twisted structure for **2** compared to that of **1**. The non-planar structure of **2** suggests the occurrence of AIE during molecular aggregation (Figure 3 and 4). Taken together, our molecular modeling results provide valuable insight into the electronic properties of molecules **1** and **2**, and help to explain their optical behavior.
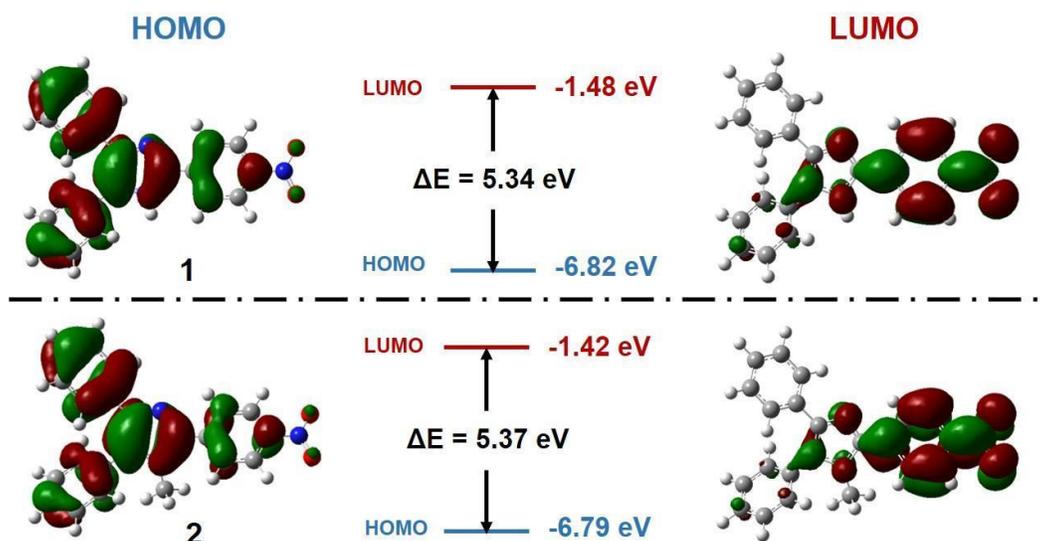
Figure 5. Molecular orbital amplitude plots of HOMO and LUMO energy levels of **1** and **2**. The molecules were optimized using M06-2X/6-31G (d,p) method.
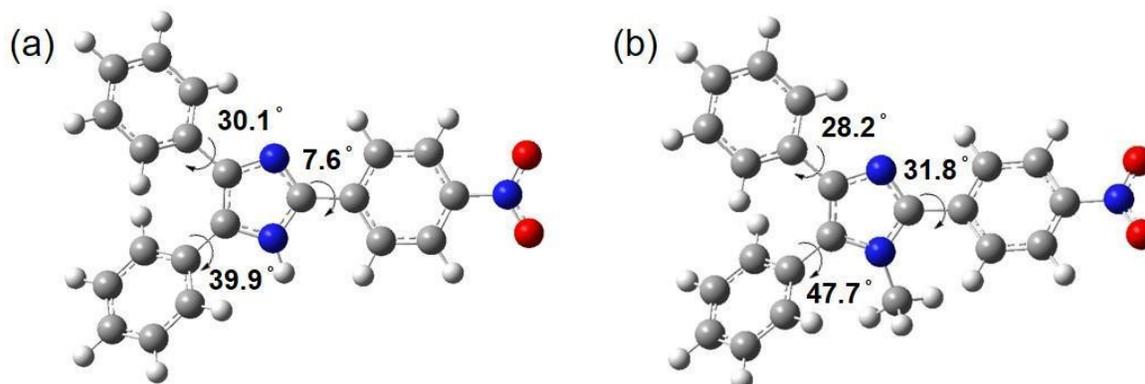
Figure 6. Molecular structures of **1** and **2**. Carbon, hydrogen, nitrogen and oxygen atoms are shown in gray, white, blue and red, respectively. The molecules were optimized using M06-2X/6-31G (d,p) method.

Conclusions

In summary, we have synthesized a novel series of imidazole-based donor-acceptor (D-A) fluorescent molecules, designated as **1** and **2**, and studied the impact of N-methyl substitution on their photophysical properties and molecular geometries. We investigated the UV-vis absorption and emission spectra of **1** and **2** in different

solvents and solid states. Furthermore, we utilized theoretical calculations to provide insights into the effect of N-methylation on the molecular structure and photophysics. By combining the experimental and theoretical results, we found that the introduction of methyl groups led to a more twisted molecular structure, which in turn resulted in the AIE properties of the material. Our research sheds light on the relationship between molecular structure and photophysical properties, providing valuable insights for the design and development of new materials with desirable optical properties.

Experimental Section

General. Materials and Instruments. Benzil and potassium tert-butoxide were obtained from Acros Organics. 4-Nitrobenzaldehyde and iodomethane were purchased from Alfa Aesar. Ammonium acetate was obtained from Sigma-Aldrich. All chemicals and reagents were commercially available and used as received without further purification. ^1H and ^{13}C NMR spectra were measured on a 400 MHz Brucker AVANCE NMR spectrometer using DMSO-d_6 as a solvent. UV-vis absorption and emission spectra were measured on JASCO V-750 and Hitachi-F-7000 fluorescence spectrophotometer, respectively.

Synthesis of compound 1. Benzil (1.00 g, 4.76 mmol), ammonium acetate (3.67 g, 47.6 mmol) and 4-nitrobenzaldehyde (1.44 g, 9.51 mmol) were dissolved in acetic acid, and the reaction mixture was refluxed for 6 h under nitrogen. After cooling to room temperature, the reaction mixture was poured into water and then subjected to dichloromethane (DCM) extraction. The resulting mixture was dried under vacuum. Subsequently, silica gel chromatography was employed to purify the crude product, using ethyl acetate/dichloromethane (1/10, v/v) as the eluent to obtain compound **1** (1.57 g, 96%). Melting point (mp)= 243-245 °C. ^1H NMR (400 MHz, DMSO-d_6): δ= 7.22-7.33 (m, 3H; ArH), 7.38-7.55 (m, 7H; ArH), 8.30-8.35 (m, 4H; ArH), 13.14 (s, 1H; NH). ^{13}C NMR (100 MHz, DMSO-d_6) δ= 124.7, 126.2, 127.4, 127.6, 128.7, 128.8, 129.0, 129.2, 130.5, 131.0, 135.1, 136.6, 138.9, 143.9, 147.0. HRMS: *m/z* (ESI$^-$) $C_{21}H_{14}N_3O_2$ calculated [M+H]$^+$ 340.10860, found *m/z* 340.10768.

Synthesis of compound 2. To a solution of compound **1** (0.500 g, 1.46 mmol) in dry THF, potassium tert-butoxide (0.214g, 1.90 mmol) was added. The reaction mixture was stirred at 0°C for an hour before iodomethane (0.270g, 1.90 mmol) was introduced at the same temperature. The mixture was then stirred overnight at room temperature. The solvent was subsequently removed and the resulting mixture was subjected to DCM extraction, followed by gravity filtration. The filtrate was concentrated under reduced pressure, leading to the isolation of compound **2** (0.517 g, 99%). mp= 209-211 °C. ^1H NMR (400 MHz, DMSO-d_6): δ= 3.58 (s, 3H, CH$_3$), 7.16-7.26 (m, 3H; ArH), 7.44-7.59 (m, 7H; ArH), 8.13 (d, *J* = 8.9 Hz, 2H; ArH), 8.39 (d, *J* = 8.9 Hz, 2H; ArH). ^{13}C NMR (100 MHz, DMSO-d_6) δ= 33.9, 124.3, 126.8, 127.0, 128.7, 129.5, 129.7 129.8, 130.7, 131.2, 132.6, 134.8, 137.2, 137.9, 145.2, 147.4. HRMS: *m/z* (ESI$^-$) $C_{22}H_{17}N_3O_2$ calculated [M+H]$^+$ 355.13153, found *m/z* 355.13156.

Computational methodology. The geometry of compounds **1** and **2** were optimized using density functional theory (DFT) with the M06-2X method at the 6-31G (d,p) level. Furthermore, an analysis of the highest occupied molecular orbital-lowest unoccupied molecular orbital (HOMO-LUMO) was conducted to elucidate the location of charge transfer within the molecules.

Acknowledgements

Supplementary Material

Spectroscopic data of ^{1}H NMR, ^{13}C NMR and HR-Mass spectra for new compounds.

References

1. Luo, J.; Xie, Z.; Lam, J. W.; Cheng, L.; Chen, H.; Qiu, C.; Kwok, H. S.; Zhan, X.; Liu, Y.; Zhu, D. *Chem. Commun.* **2001**, *18*, 1740-1741.
https://doi.org/10.1039/b105159h
2. Hong, Y.; Lam, J. W.; Tang, B. Z. *Chem. Soc. Rev.* **2011**, *40* (11), 5361-5388.
https://doi.org/10.1039/c1cs15113d
3. Zhang, J.; He, B.; Hu, Y.; Alam, P.; Zhang, H.; Lam, J. W.; Tang, B. Z. *Adv. Mater.* **2021,** *33* (32), 2008071.
https://doi.org/10.1002/adma.202008071
4. Han, P.; Xia, E.; Qin, A.; Tang, B. Z. *Coord. Chem. Rev.* **2022**, *473*, 214843.
https://doi.org/10.1016/j.ccr.2022.214843
5. Xu, L.; Yu, Y.; Shi, J.; Cui, W.; Lv, X.; Cang, M.; Sun, Q.; Xue, S.; Yang, W. *Dyes Pigm.* **2020**, *175*, 108082.
https://doi.org/10.1016/j.dyepig.2019.108082
6. Ravindra, M.; Darshan, G.; Lavanya, D.; Mahadevan, K.; Premkumar, H.; Sharma, S.; Adarsha, H.; Nagabhushana, H. *Sci. Rep.* **2021**, *11* (1), 16748.
https://doi.org/10.1038/s41598-021-96011-5
7. Wang, Y.-L.; Li, C.; Qu, H.-Q.; Fan, C.; Zhao, P.-J.; Tian, R.; Zhu, M.-Q. *J. Am. Chem. Soc.* **2020**, *142* (16), 7497-7505.
https://doi.org/10.1021/jacs.0c00124
8. Kumar, N.; Udayabhanu; Mahadevan, K. M.; Nagaraju, *J. Sci.: Adv. Mater. Devices* **2020**, *5* (4), 520-526.
https://doi.org/10.1016/j.jsamd.2020.09.004
9. Qian, J.; Tang, B. Z. *Chem* **2017**, *3* (1), 56-91.
https://doi.org/10.1016/j.chempr.2017.05.010
10. Huang, Z.; Zhou, C.; Chen, W.; Li, J.; Li, M.; Liu, X.; Mao, L.; Yuan, J.; Tao, L.; Wei, Y. *Dyes Pigm.* **2021**, *196*, 109793.
https://doi.org/10.1016/j.dyepig.2021.109793
11. Yang, Z.; Yin, W.; Zhang, S.; Shah, I.; Zhang, B.; Zhang, S.; Li, Z.; Lei, Z.; Ma, H. *ACS Appl. Bio Mater.* **2020**, *3* (2), 1187-1196.
https://doi.org/10.1021/acsabm.9b01094
12. Feng, G.; Liu, B. *Acc. Chem. Res.* **2018**, *51* (6), 1404-1414.
https://doi.org/10.1021/acs.accounts.8b00060
13. Asad, M.; Imran Anwar, M.; Abbas, A.; Younas, A.; Hussain, S.; Gao, R.; Li, L.-K.; Shahid, M.; Khan, S. *Coord.*

Chem. Rev. **2022**, *463*, 214539.
https://doi.org/10.1016/j.ccr.2022.214539

14. Lee, K.-W.; Chen, H.; Wan, Y.; Zhang, Z.; Huang, Z.; Li, S.; Lee, C.-S. *Biomater.* **2022**, *289*, 121753.
https://doi.org/10.1016/j.biomaterials.2022.121753

15. Yang, X.; Liu, Y.; Li, J.; Wang, Q.; Yang, M.; Li, C. *New J. Chem.* **2018**, *42* (21), 17524-17532.
https://doi.org/10.1039/C8NJ02616E

16. Xie, H.; Wu, Y.; Zeng, F.; Chen, J.; Wu, S. *Chem. Commun.* **2017**, *53* (70), 9813-9816.
https://doi.org/10.1039/C7CC05313D

17. Das, P.; Kumar, A.; Chowdhury, A.; Mukherjee, P. S. *ACS Omega* **2018**, *3* (10), 13757-13771.
https://doi.org/10.1021/acsomega.8b01706

18. Debsharma, K.; Santhi, J.; Baire, B.; Prasad, E. *ACS Appl. Mater. Interfaces* **2019**, *11* (51), 48249-48260.
https://doi.org/10.1021/acsami.9b17988

19. Li, S.; Shang, Y.; Wang, L.; Kwok, R. T.; Tang, B. Z. *J. Mater. Chem. C* **2016**, *4* (23), 5363-5369.
https://doi.org/10.1039/C6TC00803H

20. Yu, H.-X.; Zhi, J.; Shen, T.; Ding, W.; Zhang, X.; Wang, J.-L. *J. Mater. Chem. C* **2019**, *7* (29), 8888-8897.
https://doi.org/10.1039/C9TC01772K

21. Wang, T.; Hu, Z.; Nie, X.; Huang, L.; Hui, M.; Sun, X.; Zhang, G. *Nat. Commun.* **2021**, *12* (1), 1364.
https://doi.org/10.1038/s41467-021-21676-5

22. Duan, Y.; Liu, Y.; Han, H.; Zhang, X.; Zhang, M.; Liao, Y.; Han, T. *Spectrochim. Acta Mol. Biomol. Spectrosc.* **2021**, *252*, 119515.
https://doi.org/10.1016/j.saa.2021.119515

23. Zhu, H.; Li, M.; Hu, J.; Wang, X.; Jie, J.; Guo, Q.; Chen, C.; Xia, A. *Sci. Rep.* **2016**, *6* (1), 24313.
https://doi.org/10.1038/srep24313

24. Rančić, M. P.; Stojiljković, I.; Milošević, M.; Prlainović, N.; Jovanović, M.; Milčić, M. K.; Marinković, A. D. *Arab. J. Chem.* **2019**, *12* (8), 5142-5161.
https://doi.org/10.1016/j.arabjc.2016.12.013

25. Rodrigues, N. d. N.; Woolley, J. M.; Krokidi, K. M.; Tesa-Serrate, M. A.; Turner, M. A.; Hine, N. D.; Stavros, V. G. *Phys. Chem. Chem. Phys.* **2021**, *23* (40), 23242-23255.
https://doi.org/10.1039/D1CP03759E

26. Nabavi, S. H.; Khodabandeh, M. H.; Golbabaee, M.; Moshaii, A.; Davari, M. D. *J. Photochem. Photobiol. A:Chem.* **2018**, *354*, 127-138.
https://doi.org/10.1016/j.jphotochem.2017.05.017

27. Tian, Y.; Zhou, H.; Cheng, Q.; Dang, H.; Qian, H.; Teng, C.; Xie, K.; Yan, L. *J. Mater. Chem. B* **2022**, *10* (5), 707-716.
https://doi.org/10.1039/D1TB02066H

28. Wang, J.; Li, C.; Chen, Q.; Li, H.; Zhou, L.; Jiang, X.; Shi, M.; Zhang, P.; Jiang, G.; Tang, B. Z. *Anal. Chem.* **2019**, *91* (15), 9388-9392.
https://doi.org/10.1021/acs.analchem.9b02691

29. Zhou, T.; Zhu, J.; Shang, D.; Chai, C.; Li, Y.; Sun, H.; Li, Y.; Gao, M.; Li, M. *Mater. Chem. Front.* **2020**, *4* (11), 3201-3208.
https://doi.org/10.1039/D0QM00503G

30. Yuan, G.; Lv, C.; Liang, J.; Zhong, X.; Li, Y.; He, J.; Zhao, A.; Li, L.; Shao, Y.; Zhang, X. *Adv. Funct. Mater.* **2021**, *31* (36), 2104026.
https://doi.org/10.1002/adfm.202104026

31. Rahman, M. H.; Liao, S.-C.; Chen, H.-L.; Chen, J.-H.; Ivanov, V. A.; Chu, P. P. J.; Chen, S.-A. *Langmuir* **2009**, *25* (3), 1667-1674.
https://doi.org/10.1021/la802526d

32. Headen, T. F.; Boek, E. S.; Skipper, N. T. *Energy Fuels* **2009**, *23* (3), 1220-1229.
https://doi.org/10.1021/ef800872g

33. Chen, C.; Chi, Z.; Chong, K. C.; Batsanov, A. S.; Yang, Z.; Mao, Z.; Yang, Z.; Liu, B. *Nat. Mater.* **2021**, *20* (2), 175-180.
https://doi.org/10.1038/s41563-020-0797-2

34. Yeh, M.-Y.; Lin, H.-C. *Phys. Chem. Chem. Phys.* **2014**, *16* (44), 24216-24222.
https://doi.org/10.1039/C4CP03879G

35. Mardirossian, N.; Lambrecht, D. S.; McCaslin, L.; Xantheas, S. S.; Head-Gordon, M. *J. Chem. Theory Comput.* **2013**, *9* (3), 1368-1380.
https://doi.org/10.1021/ct4000235